

# Molecular study and analysis of organic compounds for high-performance solar cell applications

Imane El Mhamedi<sup>1\*</sup>, Zakaria El Malki<sup>1</sup>

<sup>1</sup>Materials and Systems Control (MMSC), Computer Engineering and Intelligent Electrical Systems (2ISEI) Laboratory, High School of Technology (ESTM), University Moulay Ismail, Meknes, Morocco

**Abstract.** In this study, we used time-dependent density functional theory DFT/TD-DFT methods in its B3LYP/6-311G(d,p) formalism to model and analyze various properties of conjugated organic compounds. More specifically, the targeted systems consist of a D donor unit (carbazole), an A acceptor unit (benzothiadiazole) and various donor motifs. Quantum simulation via DFT/TD-DFT has enabled us to assess their fundamental electronic structures, boundary energy levels and optical absorption properties. Using AMPS1D software, we carried out an in-depth analysis of the photovoltaic properties of six compounds associated with the PCBM acceptor. These compounds were classified into two distinct categories. In the initial section, we evaluated the energy conversion efficiency of compounds, with performances between 7% to 11%. The second section presented the addition of a PEDOT layer between the active layer and the anode, which significantly improved photovoltaic performance, reaching a maximum efficiency of 15%. These results underline the positive impact of PEDOT addition on photovoltaic conversion and its potential for organic solar cells. In conclusion, our results indicate that these compounds represent promising candidates for future applications.

## 1 Introduction

Over the last few decades, molecular materials based on  $\pi$ -conjugated systems have made significant progress. Research uncovered these systems in the 1970s thanks to the pioneering work of A. Hegger, McDiarmid and H. Shirakawa on the doping of polyacetylene [1], have since aroused growing interest and been the subject of much research [2]. Their unique physicochemical and optoelectronic properties have led to a vast field of applications in organic electronics. Today, these materials are commonly used in devices such as organic light-emitting diodes (OLEDs), organic solar cells (OSCs) and field-effect transistors [3]. The boom in these applications is linked to their remarkable characteristics, such as high electronic conductivity, easy chemical functionalization and optoselective absorption. [4]. In the emerging field of organic photovoltaics, these compounds offer substantial advantages, such as their ultra-lightweight, flexible nature. and low manufacturing cost, making them particularly attractive for renewable energy technologies [5]. Organic bulk heterojunction (BHJ) solar cells, using  $\pi$ -conjugated polymers as donors and fullerene derivatives as acceptors, have achieved high energy efficiencies [6, 7, 8]. Ongoing optimization of the morphology of bulk heterojunctions and the properties of active materials will further enhance the performance of these organic photovoltaic systems [9]. These technical advances

---

\* Corresponding author: [i.elmhamedi@edu.umi.ac.ma](mailto:i.elmhamedi@edu.umi.ac.ma)

should contribute to the wider deployment of solar energy from carbonaceous materials in renewable energy systems. The prospects for increasing yields suggest that organic photovoltaics can be used in a wide range of applications to support the energy transition. Ongoing research is aimed at advancing technologies for converting solar energy into electrical energy using organic semiconductor materials, to make them more competitive with other low-carbon energy sources. Current research in this area is crucial for the evolution of this technology towards large-scale commercialization [10].

This research focused on a family of organic molecules, in which carbazole serves as the donor unit (D), while benzothiadiazole is used as the acceptor unit (A). Various secondary donor units ( $D_i$ ) were incorporated, such as EDOT (ethylene dioxythiophene), methylthiophene, fluorene, phenylene-vinylene, vinyl and alkyne, as shown in Figure 1. The focus of this study was to analyze the structural, electronic and optical properties of these organic compounds in silico, using theoretical tools and advanced quantum simulations. To this end, we employed density functional theory (DFT), coupling the B3LYP exchange-correlation functional with a 6-311G(d,p) basis within the Gaussian 09 code. Combined with AMPS-1D simulations of their performance in solar cells, we have been able to theoretically evaluate their potential for organic photovoltaic applications.

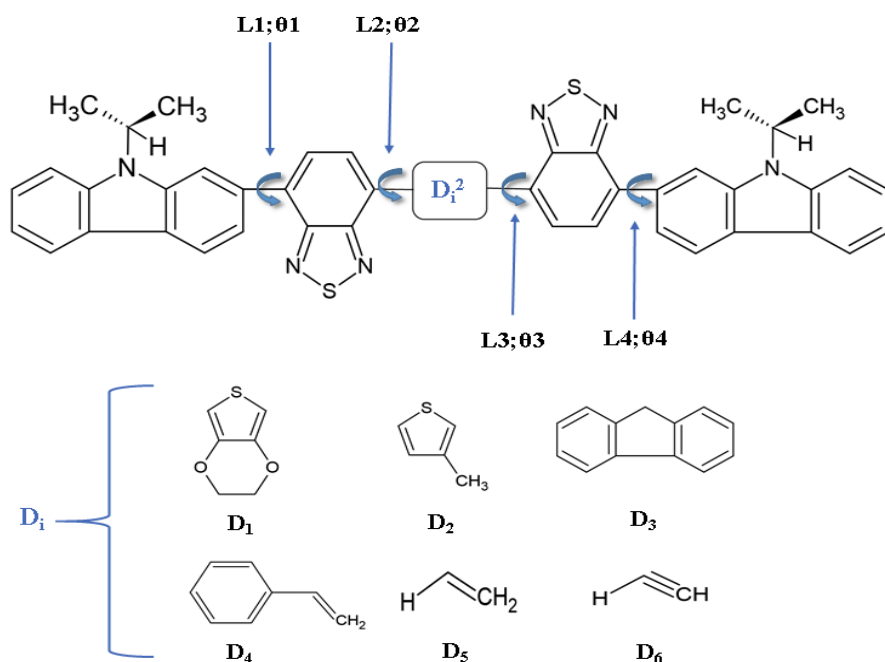


**Fig. 1.** Schematic Structures of the Studied Organic Compounds

## 2 Computational Methodology

Calculations were performed using Gaussian 09 software, with Becke's three-parameter hybrid functional (B3LYP) and the 6-311G(d,p) basis set [11] to examine neutral compounds.

The geometry of the neutral molecule was optimized, enabling HOMO, LUMO and band gap energies to be determined from the stable structure [12]. For ground-state and excited-state geometries, transition energies, wavelengths ( $\lambda_{\max}$ ), vertical excitation energy and oscillation strengths were calculated using the TD-DFT method at the B3LYP/6-311G(d,p) level.

The AMPS-1D program, which enables the analysis of one-dimensional microelectronic and photonic structures, was used for the calculations in this study. This simulation software efficiently solves the Poisson equation and the electron-hole continuity equations using the finite-difference method combined with the Newton-Raphson algorithm [13]. This numerical approach offers the possibility of analyzing model parameters that are not accessible experimentally, providing significant advantages for the study of organic solar materials.

### 3 Results and Discussion

#### 3.1 Analysis of Optimized Geometric Structures

The chemical structures of the molecules examined  $M_i (i=1-6)$  were modeled using density functional theory according to the B3LYP/6-311G(d,p) formalism. method for full optimization of their geometric parameters. Figure 2 illustrates the refined geometries of these molecules. The results, detailed in Table 1, include the intercyclic distances and dihedral angles derived from these optimized structures. Intercyclic distances range from 1.35 Å to 1.48 Å, corresponding to typical distances for single and double bonds in the carbon skeleton, indicating extensive conjugation throughout the system and promoting improved electronic conjugation. In addition, the dihedral angles  $\theta_i^\circ$  tend to be close to  $180^\circ$  for most compounds, revealing that the conjugated molecules are very planar. This increased flatness suggests the presence of more elongated  $\pi$ -conjugated systems, promoting higher intramolecular excitations (ICTs) and conversion efficiencies for the compounds examined [14, 15].

**Table 1.** Bondlengths and dihedral angles for  $M_i (1-6)$  optimized by the B3LYP/6-31G(d,p) method

Bondlengths (Å°) and dihedral angles	d1	$\theta_1$	d2	$\theta_2$	d3	$\theta_3$	d4	$\theta_4$
<b>M1</b>	1.469	172.8°	1.46	170.7°	1.45	174.1°	1.47	175.4°
<b>M2</b>	1.467	179.4°	1.45	177.7°	1.46	174°	1.47	177.5°
<b>M3</b>	1.469	-174°	1.47	-170.3°	1.47	-167.8°	1.48	-172.2°
<b>M4</b>	1.467	174.4°	1.45	173.2°	1.47	174.7°	1.48	177.7°
<b>M5</b>	1.466	174.5°	1.45	174.6°	1.45	173.5°	1.47	175.4°
<b>M6</b>	1.467	149.2°	1.42	-178.6°	1.43	179.9°	1.48	148.3°

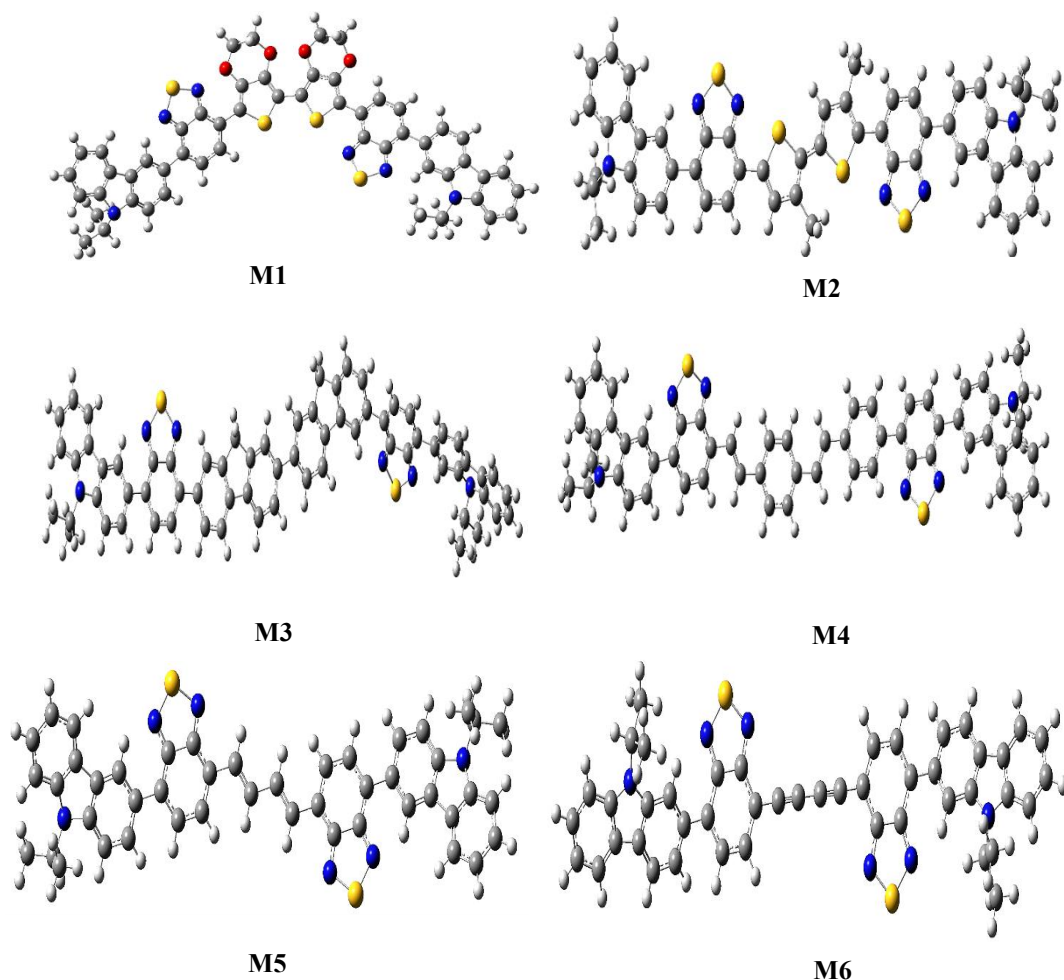


**Fig. 2.** Geometries of  $M_i$  ( $i=1-6$ ) optimized using the B3LYP/6-311G(d,p) model

### 3.2 Frontier Molecular Orbitals

The analysis of molecular frontier orbitals provides valuable qualitative information on excitation properties and energy transport within the molecule, two aspects crucial to understanding their performance [16]. As illustrated in figure 3, the study reveals that the compounds analyzed exhibit distinctly localized HOMO and LUMO orbitals. More specifically, the HOMO orbital extends homogeneously over the entire main conjugated structure, ensuring good hole mobility. Conversely, the LUMO orbital is mainly delocalized towards the inner region of the structures, hugging the benzothiadiazole groups while excluding the carbazole segments. This uneven distribution of electronic states within sheds essential light on the intramolecular charge transfer mechanisms likely to operate within these compounds, a key parameter determining their ability to absorb and convert light energy.

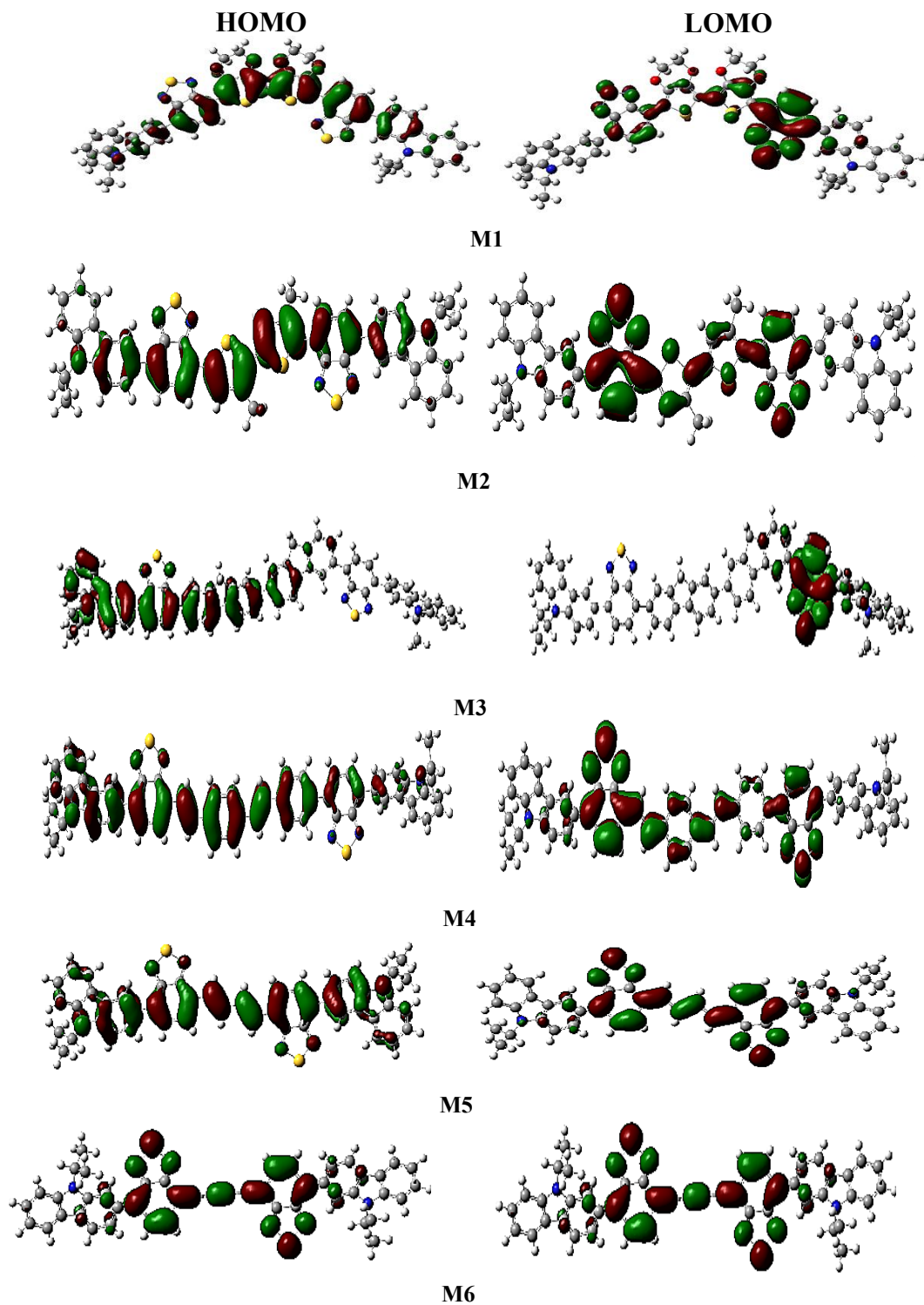


**Fig.3.** HOMO and LUMO molecular orbital mapping of Mi (i=1-6) compounds

### 3.3 Electronic Properties

In organic photovoltaic devices, the active layer consists of organic semiconductors with a bandgap generally below 2.50 electronvolts (eV). Table 2 lists the energy levels of the HOMO (EHOMO) and LUMO (ELUMO) orbitals, as well as the energy gap between the two (E<sub>gap</sub>) of the compounds studied, obtained using the B3LYP/6-31G(d,p) method. Analysis of the electronic gap values obtained for the derivatives revealed the following ascending order: M2 (2.09 eV) < M1 (2.16 eV) < M5 (2.17 eV) < M4 (2.26 eV) < M3 (2.28 eV) < M6 (2.31 eV). The M1 and M2 molecules have the lowest energy gaps, at 2.18 eV and 2.25 eV respectively. This may be explained by increased  $\pi$ -conjugation within their chemical structure. Indeed, these two derivatives have the particularity of possessing two EDOT (ethylenedioxythiophene) and methylthiophene electron-donating groups on either side of their carbon skeleton. The presence of these two groups promotes better  $\pi$ -electron delocalization along the carbon chain. This is made possible by the sulfur atom they contain, whose higher electronegativity than carbon effectively extends the conjugation length within the molecule. This extended conjugation confers on M1 and M2 derivatives their smaller electron gap compared with the other molecules studied.

**Table 2.** E<sub>HOMO</sub>, E<sub>LUMO</sub>, and E<sub>gap</sub> of M<sub>i</sub> (i=1-6) calculated using model B3LYP/6-311G(d,p)

Molecules	M1	M2	M3	M4	M5	M6
E <sub>HOMO</sub> (eV)	-4.59	-4.61	-4.99	-4.87	-4.82	-5.18
E <sub>LUMO</sub> (eV)	-2.43	-2.62	-2.71	-2.61	-2.565	-2.87
E <sub>gap</sub> (eV)	2.16	2.09	2.28	2.26	2.17	2.31

The maximum open circuit voltage (V<sub>oc</sub>) of a volume heterojunction organic solar cell is determined by the energy difference between the highest occupied molecular orbital (HOMO) of the electron donor molecule and the lowest vacant molecular orbital (LUMO) of the electron acceptor PCBM. This property is crucial for cell function. The theoretical V<sub>oc</sub> voltage can be calculated via equation (1) [17], linking V<sub>oc</sub> to the energy levels of the donor-acceptor junction. More precisely, V<sub>oc</sub> depends on the difference between the quasi-Fermi levels of the donor (EHOMO) and acceptor (ELUMO), plus a term related to their electronic affinity imbalance. The equation enables us to estimate the maximum V<sub>oc</sub> according to the electronic properties of the materials, which are crucial for organic photovoltaics.

$$V_{oc} = E_{HOMO}^{donor} - E_{LUMO}^{accepteur} - 0.3 \quad (1)$$

Analysis of Table 3 reveals positive V<sub>oc</sub> values, indicating electron transfer from the compounds to the PCBM. These results confirm the performance of the electronic injection process.

Electron affinity (EA) reflects electron acceptance capacity. We determined the EA of the compounds via the relationship [18] linking EA to the energy of the neutral and anionic states.

$$EA = E(M) - E(M^-) \quad (2)$$

The high EA values in Table 3 qualify Mi compounds as excellent electron transporters, their high affinity facilitating the acceptance of photo-generated electrons and thus charge transfer at the interface, placing these derivatives as promising candidates for organic photovoltaics. As shown in Table 3, Mi compounds exhibit high values of electron affinity EA. This analysis reveals the high electron transport capacity of these compounds.

**Table 3.**  $V_{oc}$  and EA of Mi (1-6) calculated using model B3LYP/6-311G(d,p)

Compounds	M1	M2	M3	M4	M5	M6
$V_{oc}$ (eV)	1.29	1.31	1.59	1.47	1.42	1.78
EA (eV)	1.48	1.57	1.50	1.61	1.64	1.87

### 3.4 Absorption Properties

Absorption of sunlight by the active material is an essential step in the operation of an organic photovoltaic cell. It enables the photogeneration of electron-hole pairs via the excitation of organic chromophores. These charge carriers are then dissociated and transported, thanks to the electric field and their mobility within the materials, to the electrodes where they are collected in the form of an electric current. Light absorption is therefore a decisive factor in the efficient production of the charges required for photovoltaic conversion.

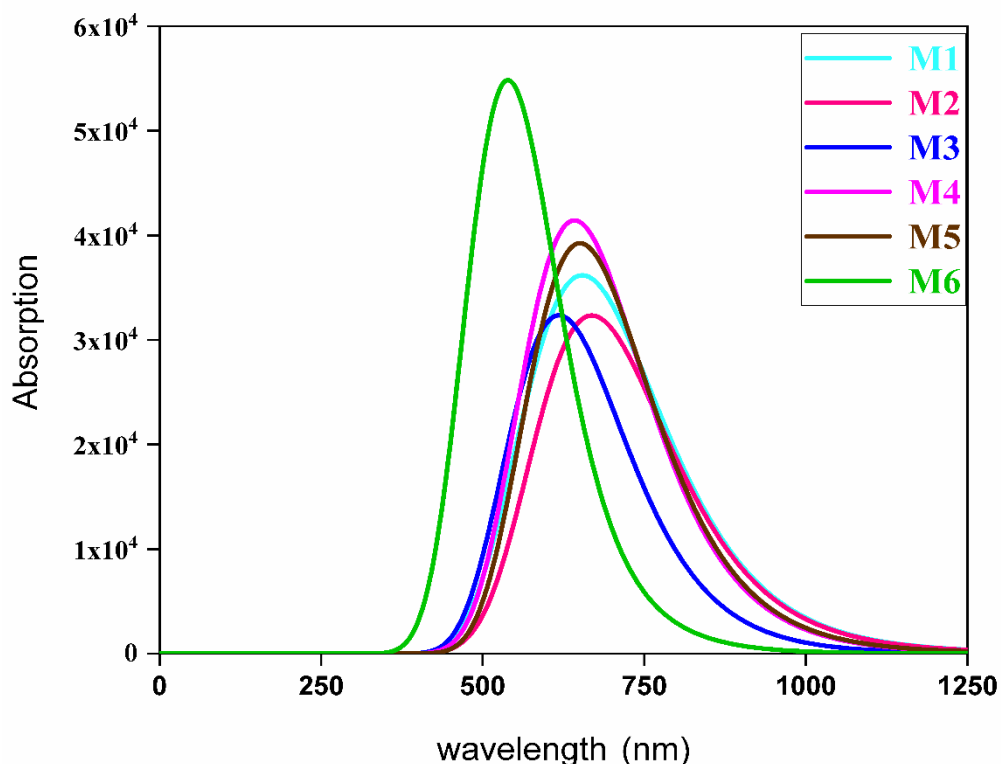


**Fig. 4.** Prediction of UV-Visible absorption spectra using time-dependent density functional theory (TD-DFT)/B3LYP/6-311G(d,p)

To assess the absorbency of Mi compounds ( $i=1-6$ ), we modeled their UV-Visible absorption spectra using TD-DFT calculations [19] based on their optimized structure B3LYP/6-311G(d,p). Table 4 shows the maximum absorption wavelengths ( $\lambda_{\max}$ ), electronic transition energies and oscillation strengths ( $f$ ) corresponding to the HOMO-1 $\rightarrow$ LUMO transitions for each molecule. Figure 4 illustrates the simulated spectra. The  $\lambda_{\max}$  follow the sequence: M6 (496 nm) < M3 (634 nm) < M5 (650 nm) < M4 (651 nm) < M2 (676 nm) < M1 (681 nm). Lying in the visible range ( $\lambda_{\max} > 400\text{nm}$ ), Compounds M1 and M2, with the highest  $\lambda_{\max}$ , show strong absorption in the visible range, due to the increased electronic donation of EDOT and methylthiophene groups. These results demonstrate the significant ability of these organic materials to absorb light over a broad spectrum, making them promising candidates for photovoltaic applications.

**Table 4.** Absorption Spectra of Mi (1-6) Obtained by TD-DFT (B3LYP/6-31G(d,p)) method

Compounds	Electronic transition	$\lambda$ (nm)	EeX (eV)	f
M1	S0 $\rightarrow$ S1	681	1.82	0.6711
	S0 $\rightarrow$ S2	598	2.27	0.2784
	S0 $\rightarrow$ S3	546	2.53	0.0441
M2	S0 $\rightarrow$ S1	676	1.83	0.7198
	S0 $\rightarrow$ S2	622	1.99	0.0781
	S0 $\rightarrow$ S3	555	2.23	0.0278
M3	S0 $\rightarrow$ S1	634	1.96	0.5641
	S0 $\rightarrow$ S2	626	1.98	0.0572
	S0 $\rightarrow$ S3	572	2.17	0.2197
M4	S0 $\rightarrow$ S1	651	1.91	0.8419
	S0 $\rightarrow$ S2	609	2.03	0.1780
	S0 $\rightarrow$ S3	559	2.22	0.0301
M5	S0 $\rightarrow$ S1	650	1.91	0.9689
	S0 $\rightarrow$ S2	583	2.11	0.0002
	S0 $\rightarrow$ S3	529	2.35	0.0001
M6	S0 $\rightarrow$ S1	496	2.49	0.0738
	S0 $\rightarrow$ S2	425	2.90	0.0475
	S0 $\rightarrow$ S3	415	2.97	1.2902

### 3.5 Photovoltaic Properties

Our study considers a bulk heterojunction organic solar cell (BHJ) composed of a donor-acceptor system. The donor material corresponds to Mi derivatives, while PCBM plays the role of acceptor. These two organic semiconductors are intimately mixed at the nanoscale, creating a bulk heterojunction (BHJ). This interpenetrating lattice architecture of the two materials has the considerable advantage of very effectively enhancing the collection of excitons generated by dissociation at the numerous donor-acceptor junctions. The stack under consideration, illustrated in figure 5, consists of an Al/Mi-PCBM/ITO multilayer structure. The Mi:PCBM active material is placed between a transparent indium tin oxide (ITO) anode and an aluminum cathode.

This two-layer configuration enables light to be brought in from the front via the transparent anode, and effectively collects opposite charges at the device terminals - the conditions required for photovoltaic conversion to work.

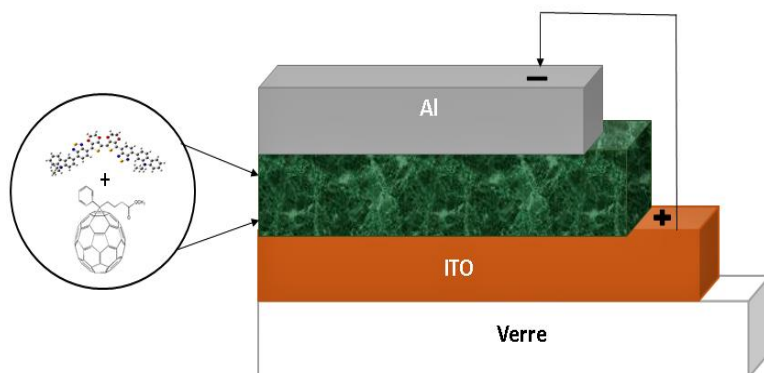


**Fig. 5.** Description of the Organic Solar Cell Design

Using the AMPS-1D method, we evaluated the photovoltaic properties of six compounds in the presence of the PCBM acceptor. The current-voltage characteristics of the devices were measured under illumination of 300 mW/cm<sup>2</sup> at room temperature for an active layer thickness of 100 nm. Figures 6 and 7 show the results for each compound respectively, as well as the effect of inserting a PEDOT layer. Table 5 records the key parameters: open-circuit voltage ( $V_{oc}$ ), short-circuit current density ( $J_{sc}$ ), form factor (FF) and yield ( $\eta$ ). In the first phase, yields ranged from 7% to 11% depending on the derivative, with a maximum for M2, probably thanks to the methylthiophene unit. In a second phase, a layer of PEDOT was introduced between the active layer and the anode. Table 5 shows the increase in  $V_{oc}$  for all compounds, leading to yields of 12% to 15%. This gain can be explained by the beneficial role of PEDOT, which improves hole collection while blocking the diffusion of undesirable elements. These results underline the positive impact of PEDOT on performance, superior to that reported for poly(3-hexylthiophene) (P3HT) [20-21].

**Table 5.** AMP1D simulated performance of organic heterojunction solar cells [Mi-PCBM]

Compounds	$J_{sc}$	$V_{oc}$	FF	$\eta$ %
M1	18.54	0.75	0.619	8.70
	21.86	1.256	0.453	14.53
M2	23.79	0.74	0.665	11.70
	19.35	1.221	0.648	15.31
M3	11.41	1.004	0.710	8.13
	22.56	1.311	0.469	13.87
M4	10.26	0.985	0.744	7.52
	21.972	1.446	0.432	13.72
M5	10.38	0.90	0.760	7.11
	21.385	1.328	0.439	12.47
M6	10.24	1.03	0.725	7.65
	21.393	1.385	0.439	12.91

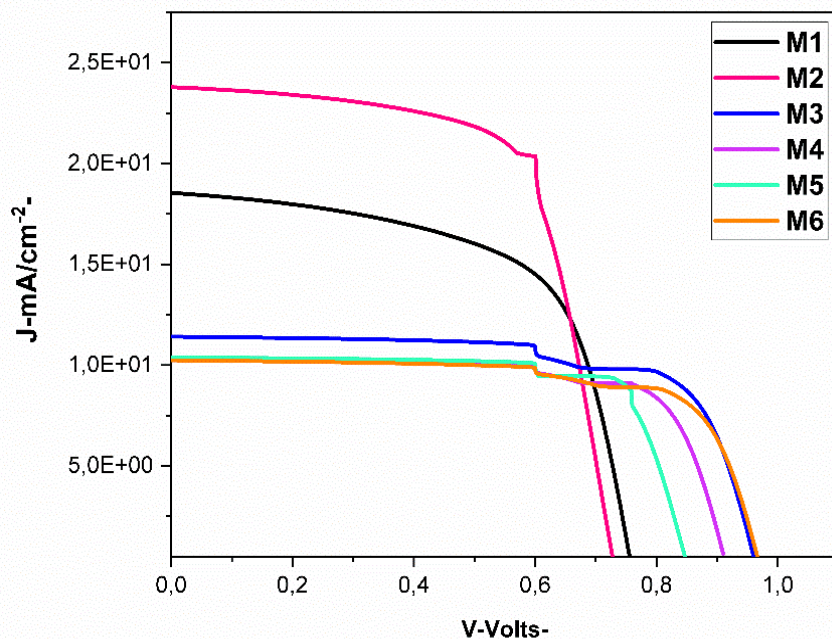


**Fig. 6.** Current-voltage curves for Mi compounds ( $i=1-6$ )

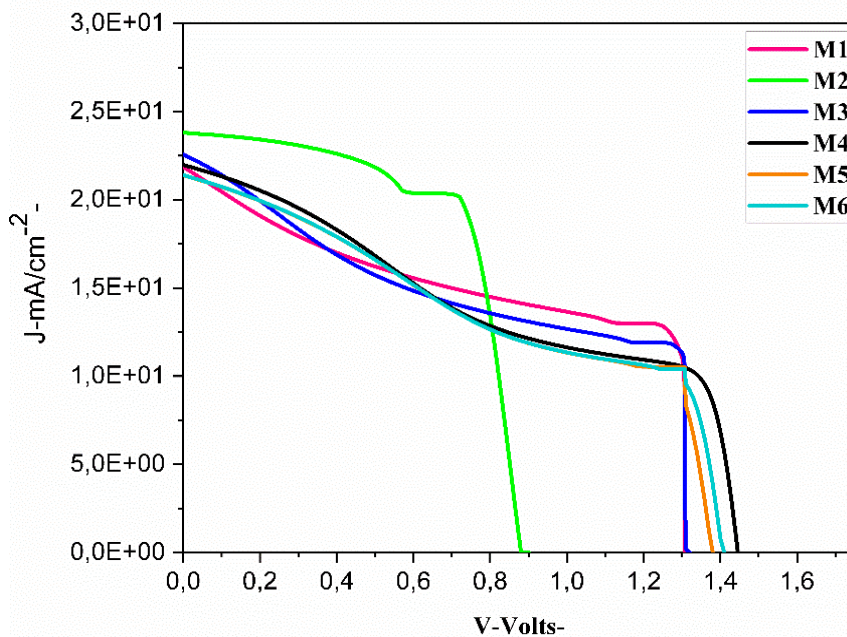


**Fig. 7.** Current-voltage curves for Mi ( $i=1-6$ ) with PEDOT insertion

## Conclusion

This study used DFT/TD-DFT methods to design and evaluate, via quantum simulation, the structural, optoelectronic and absorption properties of conjugated organic compounds based on a modular D-A-Di-A-D architecture. Calculations show the potential of these systems, integrating donor carbazole (D), acceptor benzothiadiazole (A) and various donor Di units, as active materials for interpenetrating array organic solar cells (BHJ), with LUMO levels superior to those of PCBM. Geometric optimization reveals conjugated bridge planarity, favorable to charge transfer. Spectral analysis shows extensive absorption in the visible range, testifying to their ability to efficiently capture solar radiation. The AMPS1D study of photovoltaic properties was carried out in three stages. Firstly, derivative yields varied between 7-11%. Secondly, the addition of a PEDOT layer significantly improved performance to 12-15%. These results eloquently demonstrate the benefits of PEDOT for photovoltaic conversion and position these materials as promising candidates for organic photovoltaics. They also underline the importance of optimizations such as this to progress towards more efficient and sustainable devices.

## References

1. Al-Azzawi A.G.S, Aziz S.B, Dannoun E.M.A, Iraqi A, Nofal M.M, Murad A.R, M. Hussein A (2023) A Mini Review on the Development of Conjugated Polymers: Steps towards the Commercialization of Organic Solar Cells. *Polymers*, 15, 164, <https://doi.org/10.3390/polym15010164>
2. Hmammouchi, R., Adad, A., Bouachrine, M., & Lakhlifi, T. (2013). Organic materials based on pyrazine for photovoltaic devices. *Correlation structure/electronic properties. Journal of Materials and Environmental Science*, 4(5), 752-761.
3. El karkri A, El mhamedi I, and El malki Z (2022) Prediction and Simulation of electrical and optical characteristics of an OLED based on P3BEDotBT3A organic material. *E3S Web Conf.*, 336, 00062, <https://doi.org/10.1051/e3sconf/202233600062>
4. A. He, Y. Qin, W. Dai, and X. Luo (2018) Novel D-A type dyes based on BODIPY for solution processed organic polymer solar cells. *Dye. Pigment.* 162:671-679. <https://doi.org/10.1016/j.dyepig.2018.10.068>.
5. Fichou, D., & Horowitz, G. (2001). Molecular and polymer semiconductors, conductors, and superconductors: overview. *Encyclopedia of materials: Science and technology*, 5748-5757. <https://doi.org/10.1016/B0-08-043152-6/01000-7>.
6. Son, H. J., He, F., Carsten, B., & Yu, L. (2011). Are we there yet? Design of better conjugated polymers for polymer solar cells. *Journal of Materials Chemistry*, 21(47), 18934-18945. <https://doi.org/10.1039/c1jm12388b>.
7. Mishra, A., & Bäuerle, P. (2012). Small molecule organic semiconductors on the move: promises for future solar energy technology. *Angewandte Chemie International Edition*, 51(9), 2020-2067. <https://doi.org/10.1002/anie.201102326>.
8. Zhou, H., Yang, L., & You, W. (2012). Rational design of high performance conjugated polymers for organic solar cells. *Macromolecules*, 45(2), 607-632. <https://doi.org/10.1021/ma201648t>.
9. Raftani, M., Abram, T., Bennani, N., & Bouachrine, M. (2020). Theoretical study of new conjugated compounds with a low bandgap for bulk heterojunction solar cells: DFT and TD-DFT study. *Results in Chemistry*, 2, 100040. <https://doi.org/10.1016/j.rechem.2020.100040>.

10. Taouali, W., Casida, M. E., Darghouth, A. A. M., & Alimi, K. (2018). Theoretical design of new small molecules with a low band-gap for organic solar cell applications: DFT and TD-DFT study. *Computational Materials Science*, 150, 54-61. <https://doi.org/10.1016/j.commatsci.2018.03.038>.
11. Becke, A. D. (1988). Density-functional exchange-energy approximation with correct asymptotic behavior. *Physical review A*, 38(6), 3098.
12. Ait Aicha, Y., Bouzzine, S. M., Fahim, Z. M., Zair, T., Bouachrine, M., and Hamidi M. (2014) Quantum chemical investigations study of the effect of electron donor units on the structural, electronic and optoelectronic properties of diarylthienopyrazine analogs. *Comput. Theor. Chem.* 1036: 22–30. <https://dx.doi.org/10.1016/j.comptc.2014.03.008>.
13. EL Mhamedi I, El Karkri A, and El Malki, Z (2022) Simulation of the performance of organic solar cells based on D1-BT-EDOT-BT-D2-A/PCBM structures, *E3S Web Conf.*, 336,00063. <https://doi.org/10.1051/e3sconf/202233600063>.
14. Sahu, H., & Panda, A. N. (2013). Computational study on the effect of substituents on the structural and electronic properties of thiophene–pyrrole-based  $\pi$ -conjugated oligomers. *Macromolecules*, 46(3), 844-855.
15. El malki, Z., bouachrine, M., hamidi, M., bejjit, L., haddad, M., serein-spirau, F., & montpellier, F. new organic materials based on thiadiazolothienopyrazine–dithiophene for photovoltaic applications.
16. Abram, T., Zgou, H., Bejjit, L., Hamidi, M., & BOUACHRINE, M. (2014). Design of new small molecules based on thiophene and oxathiazole for bulk heterojunction solar cells: A computational study. *J. International Journal of Advanced Research in Computer and Communication Engineering*, 2014, 4 (3), PP. 742-750.
17. Mhamedi, I. E., Karkri, A. E., Malki, Z. E., & Bouachrine, M. (2023). Simulation and analysis of electro-optical characteristics of organic compounds in organic light-emitting diodes (OLEDs).
18. El Alamy A., Bourass M., Amine A., Hamid M., Bouachrine M., (2017) New organic dyes based on phenylenevinylene for solar cells: DFT and TD-DFT investigation, *Karbala International Journal of Modern Science*. 3(2), 75-82. <https://doi.org/10.1016/j.kijoms.2017.03.002>.
19. Marques, M. A., Maitra, N. T., Nogueira, F. M., Gross, E. K., & Rubio, A. (Eds.). (2012). *Fundamentals of time-dependent density functional theory* (Vol. 837, p. 130). Berlin, Heidelberg: Springer Berlin Heidelberg.
20. EL Malki Z., Bouachrine M., Serein-Spirau F., Sotiropoulos J.-M., (2018) DFT and TD-DFT Study on the Structural, Optoelectronic and Photovoltaic Properties of Chemically Modified Donor-Acceptor Conjugated Oligomers for Organic Solar Cells, *Int. J. Adv. Res. Comput. Sci. Software Eng.* 8(12), 38–51.
21. El Mhamedi, I., El Karkri, M., El Malki, Z., & Bouachrine, M. (2023). Theoretical Study on New Conjugated Compounds of Organic Solar Cell: DFT, TD-DFT and AMPS1D. *Moroccan Journal of Chemistry*, 11(04), 11-4.